

See discussions, stats, and author profiles for this publication at: <https://www.researchgate.net/publication/258109936>

One-Parameter Model for the Oxidation of Pulverized Bituminous Coal Chars

ARTICLE in ENERGY & FUELS · JANUARY 2012

Impact Factor: 2.79 · DOI: 10.1021/ef201782n

CITATIONS

4

READS

26

5 AUTHORS, INCLUDING:



[Oskar Karlström](#)

Åbo Akademi University

15 PUBLICATIONS 70 CITATIONS

[SEE PROFILE](#)



[Anders Brink](#)

Åbo Akademi University

76 PUBLICATIONS 463 CITATIONS

[SEE PROFILE](#)



[Mikko Markus Hupa](#)

Åbo Akademi University

426 PUBLICATIONS 5,481 CITATIONS

[SEE PROFILE](#)



[Leonardo Tognotti](#)

Università di Pisa

179 PUBLICATIONS 1,996 CITATIONS

[SEE PROFILE](#)

One-Parameter Model for the Oxidation of Pulverized Bituminous Coal Chars

Oskar Karlström,^{†,*} Anders Brink,[†] Jarosław Hercog,[‡] Mikko Hupa,[†] and Leonardo Tognotti^{§,||}

[†]Process Chemistry Centre, Åbo Akademi University, Biskopsgatan 8, 20500 Turku, Finland

[‡]Institute of Power Engineering, Augustowska 36, 02-981 Warsaw, Poland

[§]Dipartimento di Ingegneria Chimica, Università di Pisa, Via Diotisalvi 2, 56100 Pisa, Italy

^{||}International Flame Research Foundation, Via Salvatore Orlando 5 57123 Livorno, Italy

ABSTRACT: In this study, the oxidation of 22 bituminous coal chars is modeled with (i) an individual activation energy for each char and (ii) constant activation energy for all the chars. Modeled burnout profiles, from 0 to 75% of burnout, are compared to experimental measurements from a 4 m isothermal plug flow reactor operating at temperatures and heating rates typical of pulverized fuel industrial combustion. The fuel and the gas rates are chosen such that temperature gradients in the radial direction and along the centerline of the reactor are minimized. In this study, the objective is to predict the burnout profiles with a model suitable for the comprehensive computational fluid dynamics (CFD) modeling of pulverized fuel boilers. Therefore, a power law model that takes into account external diffusion and apparent kinetics is used. The kinetic parameters that are used in the model are determined with a suggested multivariable optimization method. The results show that the experimental burnout profiles of the 22 individual chars are not predicted with a significantly higher accuracy using separately determined activation energy for each char than they were using a constant activation energy for all the chars. Thus, only one fuel specific parameter (i.e. the pre-exponential factor) is needed to model the burnout profiles. These findings are in agreement with some previous studies but are important considering the significant amount of experimental data and the large number of coal chars investigated using a systematic approach.

INTRODUCTION

The oxidation of pulverized coal char particles is generally predicted with models based on intrinsic kinetics or apparent kinetics.¹ In the intrinsic kinetic models, the char oxidation rate is related to the internal surface of the particle.² The internal surface area, as well as the fraction of the internal surface area that participates in the heterogeneous reaction, evolves throughout the char conversion.^{3–8} Therefore, it is complicated to take into account the internal surface area development, especially under conditions limited both by chemical kinetics and by external diffusion,⁶ that is, regime II conditions. Partly because of this, models based on apparent kinetics are widely used.⁹ Taking into account particle size distribution and various deactivation phenomena, these models can accurately predict char combustion at early, intermediate, and late combustion stages.^{10–13} Moreover, such models rely on a smaller number of fuel specific parameters than models based on intrinsic kinetics. Therefore, the models are attractive and useful for computational fluid dynamics (CFD) modeling.

In the apparent kinetic model, the oxidation rate is a function of a kinetic rate and an external diffusion rate.¹⁴ The kinetic rate is modeled using an Arrhenius expression that includes effects of both chemical reactions and pore diffusion. Ultimately, the model relies on the apparent reaction order, the apparent pre-exponential factor, and the apparent activation energy.¹⁰ The apparent reaction order, n , varies as function of temperature^{15,16} and also as a function of the properties of the coal char; for example, the rate determining steps depend on catalytic effects.¹⁷ The pre-exponential factor, A_a , includes effects of collisions between carbon and oxygen molecules and

also effects of the internal surface area. The apparent activation energy, E_a , defines the char oxidation dependence on the temperature. While the pore diffusion effects are not explicitly included in the apparent kinetic model, E_a differs from the intrinsic activation energy, E_i . Under regime II conditions, it has been suggested that the value of E_a is about half of the value of E_i .^{1,18,19} This relationship can be derived for simple particle shapes.¹⁹ In general, E_a values have been determined to be around 50–100 kJ/mol, and E_i values are around 100–200 kJ/mol.^{1,2,14,18,20–25} Moreover, correlations for E_a as function of the parent coals properties have been suggested.^{1,21,26} Fu et al., however, questioned whether E_i is dependent on the parent coals properties.²⁷ They showed that calculated kinetic rates of bituminous coal char and anthracite chars were relatively similar when both char dependent E_i and a constant E_i of 180 kJ/mol was considered. They emphasized that E_i mainly is affected by chemical factors, such as carbon type, active sites, and catalytic effects that have similar influences both on bituminous coal char and anthracite chars. For lignite chars, the mineral matter has an important influence on E_i , which therefore differs from E_i of bituminous coal chars and anthracite chars.¹⁷ Moreover, Zolin et al. suggested the intrinsic activation energy to be constant for various types of coal chars at regime I conditions, according to thermogravimetric analysis (TGA) tests.²⁸ However, physical factors influencing the oxidation are char specific, also for chars derived from parent coals of similar

Received: November 15, 2011

Revised: January 7, 2012

Published: January 9, 2012



Table 1. Coals, Experimental Conditions, Determined Activation Energy, and Differences of Object Function

coal	FC % ^a	A % ^b	d/ ρ ^c	exptl. condit. ^d	E_a ^e	A_a ^e	A_{74} ^e
Columbian coal	59	11	44/477	1223/4,8,12 1473/4 1673/4	66	0.131	0.264
Dawmill fine	61	19	40/414	1223/5 1473/5 1673/5	71	0.304	0.410
Douglas prem. (a.f.) ^f	69	12	40/500	1223/4,8,12 1473/4 1673/4,8,12	67	0.143	0.254
Douglas prem. (a.f.)	69	12	36/667	1223/4,8,12 1473/4 1673/4,8,12	82	0.564	0.298
economy	70	16	61/642	1223/4,6,8,12 1373/8 1473/6 1573/4 1673/3	87	1.430	0.453
El Cerrejon	61	6	39/431	1123/5 1473/5 1673/5	71	0.259	0.329
Enel coal 2001	59	11	35/552	1223/4,8,12 1473/4 1673/4	53	0.070	0.471
Fettmuss	71	4	71/792	1223/11.9 1473/6 1673/3.4	91	2.997	0.732
Genesee	63	28	64/532	1223/12 1373/8 1473/6 1573/5 1673/3	53	0.457	2.479
Gottelborn	63	10	39/407	1123/5 1473/5 1673/5	59	0.077	0.286
Gottelborn <150	62	9	67/420	1223/5 1473/5 1673/3	99	7.013	0.842
Kellingley 45	67	19	21/622	1223/4,8,12 1473/4 1673/4	90	1.070	0.254
Kellingly coarse	62	8	72/420	1223/4,8,12 1473/4 1673/4,8,12	48	0.073	0.531
Kleinkopje	72	15	41/604	1123/5 1473/5 1673/5	56	0.056	0.249
Kleinkopje	68	14	19/579	1223/4,6,8,12 1473/4 1673/4	99	1.612	0.167
Middelburg fine	68	17	42/560	1223/5 1473/5 1673/5	62	0.103	0.275
Polish	66	12	70/415	1123/5 1473/5 1673/5	59	0.112	0.349
Polish	67	4	38/480	1223/4,8,12 1473/4 1673/4	85	1.038	0.394
Polish	64	9	24/519	1223/4,6,8,12 1473/4 1673/4	90	1.103	0.249
Polish 5600	63	15	107/578	1223/4,6,8,12 1373/8 1473/6 1573/4 1673/3	54	0.149	0.968
South African	63	11	42/544	1223/4,8,12 1473/4 1673/4	68	0.332	0.564
Spitsbergen	60	25	57/691	1223/12 1473/6 1673/3	62	0.277	0.747

^aFixed-carbon content of parent coal (daf). ^bAsh-content of parent coal (db). ^cMean-mass diameter of char particles, d (μm); particle density, ρ (kg/m^3). ^dExperimental conditions, for example, for Columbian coal char experiments have been performed at the following reactor temperatures and oxygen concentrations in the gas: 1223 K/4% O_2 , 1223 K/8% O_2 , 1223 K/12% O_2 , 1473 K/4% O_2 and 1673 K/4% O_2 . ^eOptimized activation energy, E_a (kJ/mol) and pre-exponential factor, A_a ($\text{g}/(\text{m}^2 \text{ s Pa})$). A_{74} is the optimized pre-exponential factor with a constant apparent activation energy of 74 kJ/mol. ^fa.f.: as fired

rank.^{1,29} As a consequence, it is unclear to what extent E_a can be treated as independent of the parent coals properties. However, it has surprisingly not been shown whether E_a can be treated as constant under relevant combustion conditions for a large number of coal chars of similar rank.

In the current study, the oxidation of 22 bituminous coal chars is modeled using an apparent kinetic model with (i) individual E_a for each char and (ii) constant E_a for all chars. Modeled burnout of the chars, from 0 to 75% of burnout, is compared to experimental measurements from a 4 m drop tube reactor, named isothermal plug flow reactor (IPFR), at combustion temperatures and heating rates typical of a practical pulverized fuel systems. The experimental data used in this study come from the IFRF solid fuel database.³⁰ The kinetic parameters are optimized with a multivariable optimization method.²⁵ The main objective of the study is to investigate whether it is possible to model burnout profiles of the chars using constant apparent activation energy, while choosing the reaction order to be constant for the chars. In such case, only one fuel specific input parameter, that is, A_a , is required to predict the char oxidation burnout profiles.

■ EXPERIMENTAL SECTION

Table 1 lists the 22 bituminous coal chars that were investigated. The fixed-carbon content of the parent coals varied between 59 and 72%, and the initial mean char particle diameters varied between 19 and 107 μm . The experimental data were taken from the IPFR solid fuel database, which contains the ultimate and proximate analyses, initial diameters, and densities of the 22 chars and their parent coals. Table 1 also shows the char particle densities, including both the true char density and the porosity of the particles. In addition, the database contains burnout as a function of time for the parent coals and for the chars derived from the coals. The burnout profile experiments were

performed in a drop tube reactor named the isothermal plug flow reactor (IPFR). The experimental setup has been described in previous work.^{25,30} A brief description is given below.

In the IPFR, the thermal conversion takes place in a 4 m long vertical tube. The tube contains eight electrically heated modules. The parent coals were devolatilized in N_2 at 1473–1673 K, usually with a small amounts of oxygen (less than 0.5%), to prevent tar condensation on char particles. In the devolatilization tests, the parent coal particles were fed from the top of the reactor system by a vertical probe, and the samples were collected by a vertical movable probe, consisting of water cooled jacket and a nitrogen quench. The remaining chars were collected for the combustion tests: the char was fed through different horizontal ports situated along the height, and the samples were quenched at the bottom of the system. The char oxidation experiments were generally performed at gas temperatures of 1223–1673 K (see Table 1). For the considered particle sizes, this temperature interval is particularly interesting for regime II conditions. For each char, the particle burnout fractions at different residence times are obtained using an ash tracer method: the measured ash contents are related to the initial ash contents of the original chars. The gas velocity in the reactor was between 3.5 and 6 m/s, and the inner diameter of the combustion chamber is 150 mm, giving Reynolds numbers around 3000. The fuel and the preheated gas flow rate were chosen such that a significant temperature increase in the surrounding gas and at the furnace walls is avoided. Moreover, the rates were set to achieve a maximum relative oxygen drop of 10% over the reactor length. The fuel flow rate was around 0.1 kg/h, and the preheated gas flow was around 40–80 $\text{m}_\text{N}^3/\text{h}$. For each set of experimental conditions, 4–7 fuel samples were taken. The experimental conditions of the combustion tests are shown in Table 1.

■ MODEL AND DETERMINATION OF KINETIC PARAMETERS

Model. The model used to predict the burnout profile of the 22 bituminous coal chars in the IPFR is based on apparent

kinetics and external diffusion:^{2,14}

$$\frac{dm_p}{dt} = S_p k \left(P_{O_2, \infty} - \frac{dm_p}{dt} \frac{1}{S_p D} \right)^n \quad (1)$$

where

$$k = A_a \exp(-E_a/RT_p) \quad (2)$$

and

$$D = C \frac{[(T_p + T_\infty)/2]^{0.75}}{d_p} \quad (3)$$

This model is frequently used, because it requires few input parameters but is still able to give accurate char oxidation predictions.^{2,10,12,21,25} In eqs 1–3, m_p is the mass of the particle; S_p is the external surface area of the particle; D is the external diffusion rate coefficient; P is the partial pressure; k is the apparent kinetic rate; A_a is the apparent pre-exponential factor; E_a is the apparent activation energy; n is the apparent reaction order; C is a diffusion constant ($= 5 \times 10^{-12} \text{ s/K}^{0.75}$); and d_p is the external diameter. The particles are considered to be spherical; thus, $S_p = \pi d_p^2$, and the diameter evolution is modeled according to

$$\frac{d_p}{d_{p,0}} = (1 - U)^\alpha \quad (4)$$

Here, α is the burning mode, and U is the fractional degree of burnout. The temperature of the char particle is calculated from the heat balance of the particle:

$$m_p c_p \frac{dT_p}{dt} = h S_p (T_\infty - T_p) - f_h \frac{dm_p}{dt} H_{\text{reac}} + S_p \epsilon_p \sigma (\theta_R^4 - T_p^4) \quad (5)$$

where c_p is the heat capacity of the particle; h is the convective heat transfer coefficient ($= Nu/k_\infty d_p$); f_h is the fraction of the heat that the particle absorbs from the heat released by the surface reaction H_{reac} ; ϵ_p is the emissivity of the particle surface; σ is the Stefan–Boltzmann constant; and θ_R is the radiation temperature. For clarification, the following points are presented:

- (i) The kinetic parameters incorporate effects such as pore diffusion, internal surface area development, and deactivation besides the pure chemical effects. However, it has been shown that the model can be used at similar conditions as in the present study without explicitly taking these factors into account.^{11,12,25}
- (ii) The burning mode, α is assumed to be 0.25 for all the chars. Thus, both the density and the diameter decrease throughout the conversion, and the formation of possible ash layers is not considered. It is important to note that α is a function of the combustion conditions, particle size, and reactivity. However, Ballester et al.¹² shows that the predicted char oxidation rates are significantly influenced by the value of α only at high degrees of conversion, which is out of the scope of this study.
- (iii) The model can be used up to 75% of conversion by assuming the particles to be monosized.²⁵ Therefore, degrees of conversion up to 75% are considered in this study.

- (iv) The Stefan flow is not taken into account, because it generally has a small influence for the considered particle sizes, oxygen concentrations, and reaction temperatures.³¹
- (v) The single char oxidation product is assumed to be CO, even if there, at least at the lowest temperature, should be some CO₂ formation.³²
- (vi) The temperatures of the bulk gas and of the furnace walls are assumed to be constant in the model; reactor characterizations have shown that the temperatures are constant over a wide range of operating conditions and residence times.
- (vii) The following parameter values are used: $c_p = 2300 \text{ J/(kg K)}$; $f_h = 1$;¹⁴ $\epsilon_p = 0.85$.⁶
- (viii) In a previous study, it was shown that the apparent reaction order is close to one at 1223 K for 10 of the 22 chars investigated in the present study.²⁵ However, the apparent reaction order varies as a function of temperature.^{15,16} Nevertheless, it is obvious that the value of the apparent reaction order influences the apparent activation energy.¹⁰ Therefore, the apparent reaction orders of the investigated chars must be fixed in order to justify a comparison of the activation energies. In the present study, the apparent reaction order is chosen to be one for the 22 chars.

Determination of Kinetic Parameters. The kinetic parameters are determined with a multivariable optimization approach used in a previous study,²⁵ by minimizing the residuals between the modeled and experimental burnout profiles according to the least-squares objective function

$$f_{\min} = \left(\frac{1}{j_{\max} k_{\max}} \sum_k \sum_j f_{j,k}^2 \right)^{1/2} \quad (6)$$

where

$$f_{j,k} = (U_{\text{mod}} - U_{\text{expt}})_{j,k} \quad (7)$$

Here, the subscript mod stands for modeled and expt for measured; j, k refers to the j th sampled point in the experiments for the k th experimental test condition. For the above-mentioned reasons, all burnout points U_{expt} below 75% are included in the optimization. In the optimization, A_a is constrained to be positive using the transformation $A_a = \exp \theta$, where θ is between -25 and $+5$. The apparent activation energy E_a is constrained to be between 10 and 200 kJ/mol. The joint optimization of θ and E_a is conducted separately for each char with the apparent reaction order fixed at 1.

Determination of Constant Activation Energy. To determine the constant E_a that best suits the 22 chars, the following objective function is defined:

$$F = \frac{1}{22} \sum_{\text{char}=1}^{22} f_{\min}(E_a) \quad (8)$$

Thus, for each of the 22 chars, A_a is optimized for a constant E_a (10 kJ/mol). The procedure is then repeated for various constant E_a (11, 12, ..., 200 kJ/mol). The minimum value of F gives the optimum constant E_a that best suits the 22 chars.

RESULTS AND DISCUSSION

Figure 1 shows the apparent activation energies for the 22 chars where both A_a and E_a have been optimized separately for each

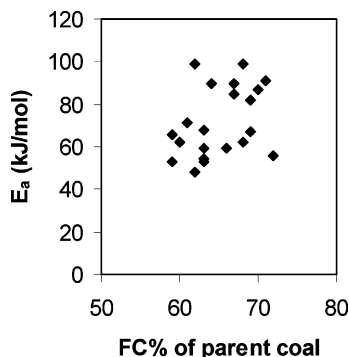


Figure 1. Apparent activation energies of 22 bituminous coal chars.

chars. The activation energies are plotted as a function of the fixed-carbon content of the parent coals. There is no obvious relationship between the reaction order and the fixed-carbon content of the parent coals. The activation energies lie between 48 and 99 kJ/mol and are listed in Table 1. These values are in agreement with reported values and are typical for regime II combustion.^{1,2,10,12,25} However, it is necessary to investigate to what extent the external diffusion influences the conversion rates. Therefore, fractions of external mass transfer control have been calculated by comparing modeled conversion rates to rates controlled by external mass transfer ($A_a \rightarrow \infty$ in eq 2). The maximum values of these fractions are generally between 0.01 and 0.05 at 1223 K. At this temperature, the highest value was observed for the Genesee char, that is, 0.27. Correspondingly, the mass transfer fractions are generally around 0.10–0.20 at 1673 K. Also at this temperature, the highest value was observed for the Genesee char, that is, 0.38. Thus, it is likely that the combustion conditions for the 22 chars are within regime II. It is important to note that all the kinetic parameters have been determined using the particle temperatures according to eq 5. The maximum particle temperature is generally around 20–50 K above the reactor temperature at 1223 K and around 100–200 K above the reactor temperature at 1673 K. Moreover, it is important to note that these temperature increases are strongly dependent on the particle size and reactivity.

Figure 2 illustrates a contour diagram of A_a and E_a for a Polish coal char; the contours correspond to the values of the

objective function. The optimum E_a is 85 kJ/mol. However, the figure shows that a range of parameter combinations of A_a and E_a can be used to yield a similar value of the objective function, as in the optimum case.

To quantify the objective function, Figure 3 presents modeled and experimental burnout profiles of the Polish coal char with various kinetic parameter combinations yielding in different objective functions. In the optimum case, the objective function is 0.065, and the corresponding E_a is 85 kJ/mol. For $E_a = 73$ kJ/mol, the objective function increases to 0.077; for $E_a = 57$ kJ/mol, the objective function increases to 0.115; and for $E_a = 36$ kJ/mol, the objective function increases to 0.164. It can be seen that, for the two best cases ($E_a = 85$ kJ/mol and $E_a = 73$ kJ/mol), the burnout predictions are accurate for $U < 0.75$, as excepted.^{11,12,25} Using $E_a = 57$ kJ/mol, the burnout predictions may be considered adequate. However, the modeled burnout profiles deviate significantly from the experimental burnout profiles using $E_a = 36$ kJ/mol, especially at the highest reactor temperature, that is, 1673 K. Nevertheless, it is obvious that range of activation energies can be used in the model to adequately fit the experimental burnout data for the Polish coal char.

Figure 4 displays the mean objective function as a function of the constant apparent activation energy according to eq 8. The optimum constant apparent activation energy is 74 kJ/mol. Note that the derivative of the mean objective function curve is near zero in the proximity of 74 kJ/mol, which means that a constant E_a could equally well be chosen in the interval of 70–80 kJ/mol for the 22 coal chars. This analysis has also been performed using other reaction orders. In the figure, the mean objective function curve is displayed for $n = 0.5$. The mean objective function is slightly higher, and the value of constant apparent activation energy decreases to 64 kJ/mol. Figure 5 illustrates the objective functions for the 22 coal chars when E_a is separately optimized for each char, and when $E_a = 74$ kJ/mol for all the chars. Note that the pre-exponential factors are optimized separately for each char. Generally, the objective functions are similar in both cases, implying that the constant activation energy of 74 kJ/mol is appropriate. It should, however, be noted that the objective functions for one of the chars are comparatively high: the objective function of the Dawmill coal char is 0.283. Figure 6 shows modeled and experimental burnout profiles for the Dawmill coal char. In the figure, an experimental outlier explains the high objective function, because the burnout predictions are accurate for the remaining experimental data points below 75% of burnout.

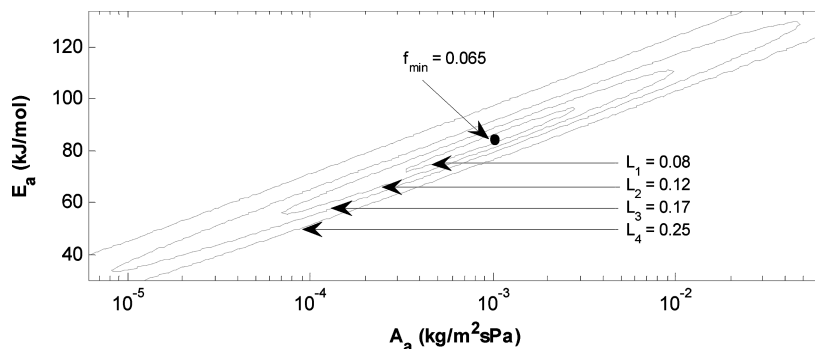


Figure 2. Contour diagram of the apparent pre-exponential factor and apparent activation energy of a Polish coal. The values indicated on the contours correspond to the values of the objective function. The minimum is marked with a filled circle.

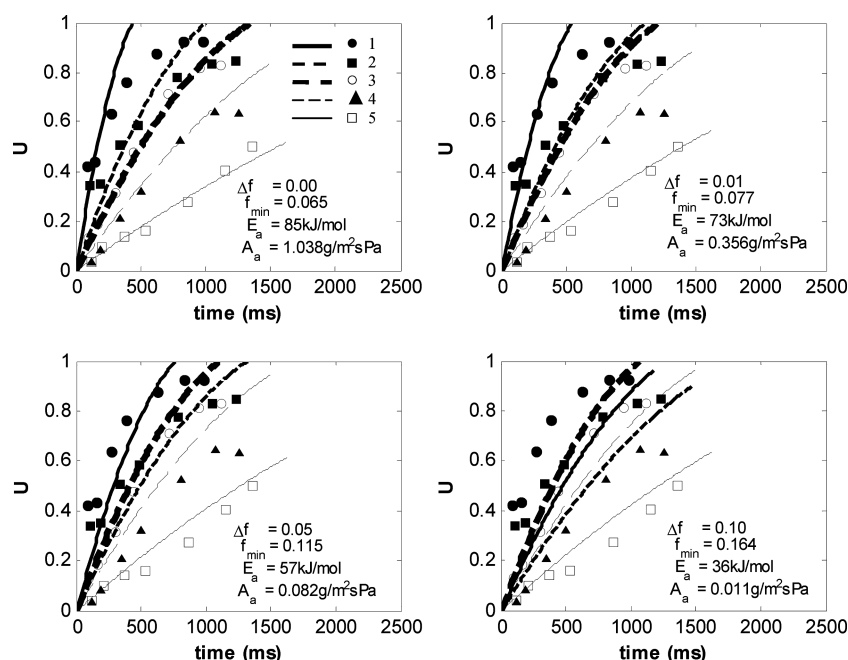


Figure 3. Modeled and experimental burnout versus residence time with various apparent reaction orders for a Polish coal char. The symbols represent the experimental data, and the lines represent the modeled data. Conditions 1–5 refer to (1) 1673 K/4% O₂, (2) 1473 K/4% O₂, (3) 1223 K/12% O₂, (4) 1223 K/8% O₂, and (5) 1223 K/4% O₂.

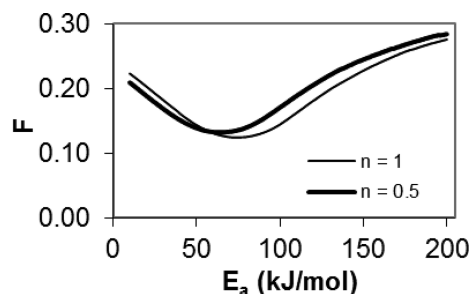


Figure 4. Mean objective function as a function of the apparent activation energy of 22 bituminous coal chars with apparent reaction order of 0.5 and 1.

To test whether there is any statistical difference in the two groups of objective functions, the following hypothesis is tested: the expected value of the objective functions with $E_a = 74$ kJ/mol (population 1) is higher than the expected average value of the objective functions with E_a optimized separately for each char (population 2). Here, the expected average value of population 2 is assumed to be equal to the mean value of population 2, that is, 0.114. To test the hypothesis, a one-sided confidence interval is calculated for population 1:

$$I_{\mu} = \left(\bar{x} - \frac{t_{\alpha}(v) \cdot s_x}{\sqrt{n}}; \infty \right) \quad (9)$$

where \bar{x} is the mean value of population 1, 0.126; t_{α} is the t -quantile; s_x is the standard deviation; n is the size of the

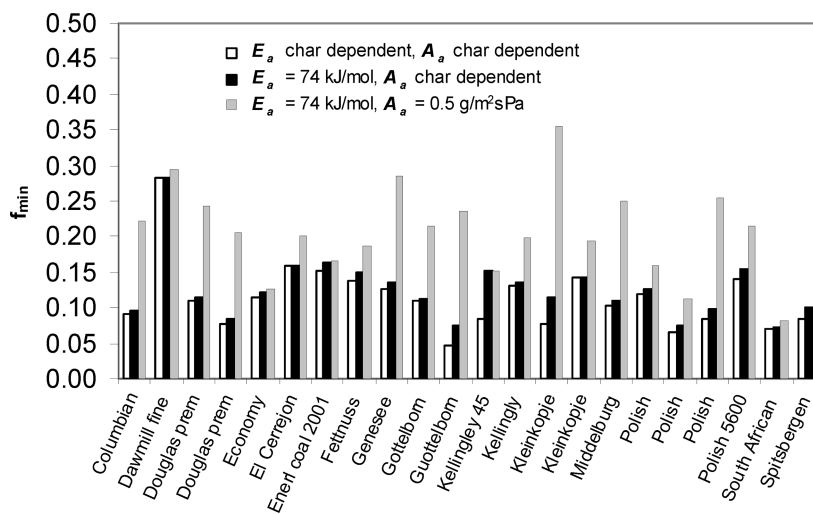


Figure 5. Minimum values of objective functions using the optimized activation energies for 22 chars, constant a activation energy for the 22 chars, and constant activation energy and constant pre-exponential factor for the 22 chars.

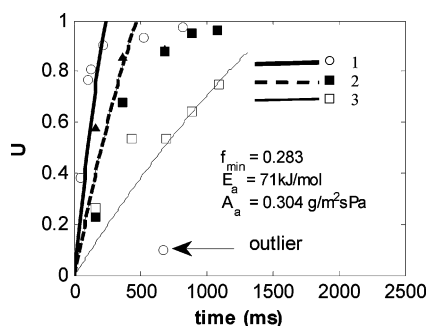


Figure 6. Modeled and experimental burnout versus residence time for a Dawmill char. The symbols represent the experimental data, and the lines represent the modeled data. The outlier experimental data point is marked with a circle. Conditions 1–3 refer to (1) 1673 K/5% O₂, (2) 1473 K/5% O₂, and (3) 1223 K/5% O₂.

population; and $\nu = n - 1$. The confidence interval equals to $I_\mu = (0.109; \infty)$ with a significance level of 0.05. According to the confidence interval, the expected value of population 1 can be smaller than the expected average value of population 2, and consequently, the hypothesis cannot be accepted.

With a constant E_a and n , it is interesting to compare A_a of the 22 chars, because A_a in such a case is the single fuel specific parameter. In such a case, the difference in A_a corresponds to the difference in the kinetic rate at a given temperature: with $A_a = 0.2 \text{ g/(s m}^2 \text{ Pa)}$ for one char and with $A_a = 1 \text{ g/(s m}^2 \text{ Pa)}$ for another char, there is a difference of a factor 5 in the kinetic rates at any given temperature. Figure 7 shows A_a (with

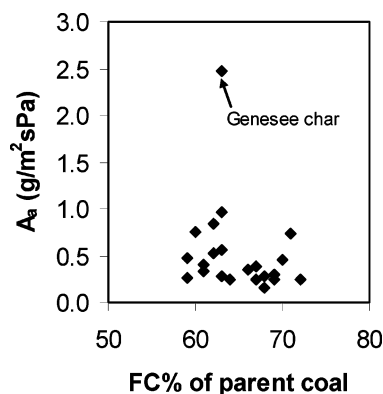


Figure 7. Apparent pre-exponential factors of 22 bituminous coal chars with a constant apparent activation energy of 74 kJ/mol for each char.

constant E_a of 74 kJ/mol) of the 22 chars as a function of the fixed-carbon content of the parent coals. For 21 of the 22 chars A_a values vary between 0.2 and 1 g/(s m² Pa), while A_a of the Genesee char is 2.5 g/(s m² Pa). As a consequence, the kinetic rate for the Genesee char is more than 12 times higher than the coal chars with the lowest reactivity, that is, the lowest value of A_a . Because of the high reactivity of the Genesee char, it is relevant to compare the experimental oxidation rates to rates controlled by external diffusion, that is, regime III combustion. Figure 8 shows modeled and experimental burnout profile of the Genesee char with constant E_a of 74 kJ/mol and with external diffusion control ($A_a \rightarrow \infty$ in eq 2). The figure shows that the oxidation is close to mass-transfer controlled, which is surprising considering the mean char particle size (64 μm) and the reactor temperatures (lowest is 1223 K). For a 100 μm coal char particle the diffusion limit is generally thought to be

around 1700–2300 K.^{10,21,23,33,34} Nevertheless, the oxidation reactivity is significantly higher for the Genesee coal char than for the remaining 21 chars.

It should be remarked that A_a is determined by several factors such as structural parameters and the collisions between oxygen and carbon. Moreover, A_a is influenced by intraparticle oxygen pressure gradients because the apparent kinetic rate is related to the oxygen pressure at the external surface of the particle, while the heterogeneous reactions on the pore walls is a function of the local oxygen concentrations. To demonstrate the influence of A_a on the objective function, the objective functions of the 22 chars have been calculated with $A_a = 0.5 \text{ g/(s m}^2 \text{ Pa)}$ for the 22 chars, because most of A_a is in the proximity of 0.5 g/(s m² Pa) for the chars. In Figure 5, the objective functions with all the kinetic parameters fixed for the 22 chars are illustrated, that is, $A_a = 0.5 \text{ g/(s m}^2 \text{ Pa)}$, $E_a = 74 \text{ kJ/mol}$, and $n = 1$. The figure shows that the objective functions, and thus the difference in the fits between modeled and experimental data, increase significantly when A_a is fixed compared to when A_a is char specific. Therefore, it is obvious that A_a is very sensitive for achieving a high accuracy in the char oxidation predictions. The deviations in the pre-exponential factors of the chars with constant E_a arise from several factors, as mentioned. However, a significant scatter in the internal specific surface areas have been reported for bituminous coal chars.^{1,2,29} Therefore, it is possible that the deviations in the pre-exponential factors can be justified by differences in the specific internal surface areas or by differences in the char morphologies as suggested by Brix et al.³⁵ One interesting point is that the internal specific surface area of char particle changes throughout the conversion under regime II conditions.^{1,3,4,11,29} In this study, however, the pre-exponential factor is kept constant up to 75% of conversion. In fact, Ballester and Jimenéz showed that by taking variations in particle sizes into account it possible to model the char oxidation burnout until around 95% of conversion with a constant pre-exponential factor.¹² Therefore, it is likely that the internal surface area evolution plays an important role only at very high degrees of conversion under regime II conditions, because there is a direct relationship between the internal specific surface area and the apparent pre-exponential factor.²

CONCLUSIONS

Burnout profiles, from 0 to 75% of burnout, of 22 bituminous coal chars were modeled with (i) individual apparent activation energy for each char and (ii) constant apparent activation energy for each char. Modeled burnout data was compared to experimental measurements from an isothermal plug flow reactor operating at 1223–1673 K. The following conclusions can be drawn:

The activation energies were between 48 and 99 kJ/mol when both the activation energy and the pre-exponential factor was optimized separately for each char.

The constant apparent activation energy that best suited the 22 chars was 74 kJ/mol.

The apparent pre-exponential factors of the 22 chars varied significantly when the apparent activation energy was chosen to be 74 kJ/mol. For the most reactive char, the apparent pre-exponential factor, and thus the kinetic rate, was more than 12 times higher than the apparent pre-exponential factor of the least reactive char. Despite the very high reactivity, the combustion was not solely limited by external diffusion.

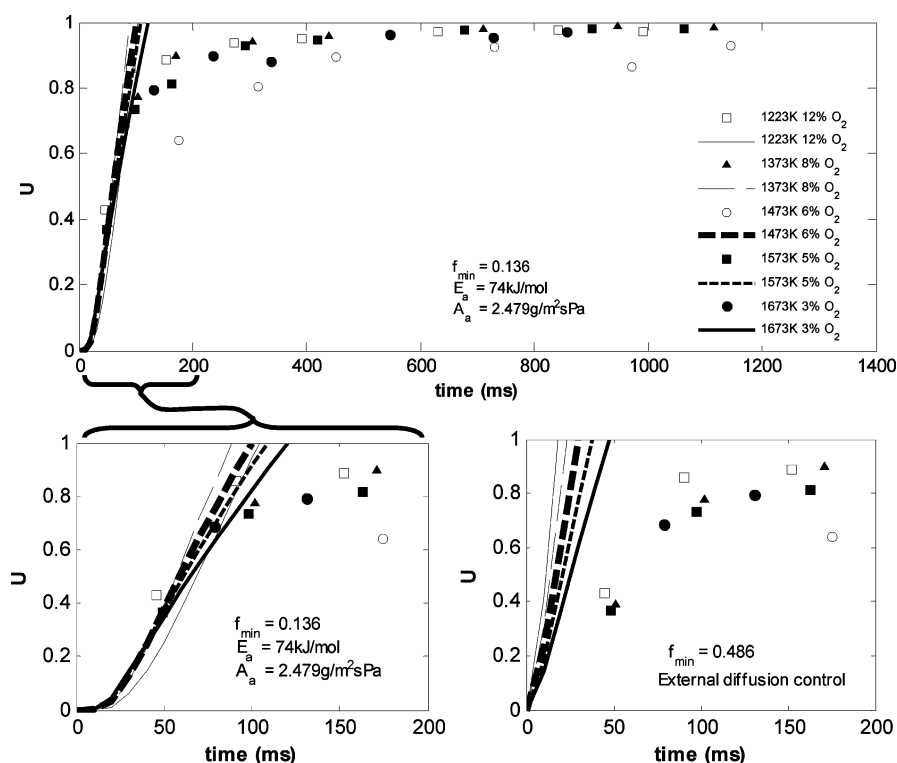


Figure 8. Modeled and experimental burnout versus residence time for a Genesee char. The symbols represent the experimental data, and the lines represent the modeled data.

There was no significant difference in the fits between the modeled and the experimental data for the 22 chars when the activation energies were separately optimized for the chars and when a constant activation energy was used for the chars. Thus, only one char specific kinetic parameter is required to predict the burnout profiles of the bituminous coal chars.

Because most comprehensive CFD codes for the modeling of pulverized fuel combustion are using simple kinetic/diffusion models, these findings provide additional confidence in achieving predictivity, at least for the main combustion regions of the boiler where most of the heat is released by pulverized fuel. This is not the case for late stages of char oxidation, which should be treated by means of a more detailed and uncoupled postprocessed approach to predict carbon in ash or mineral matter effects and transformations.

AUTHOR INFORMATION

Corresponding Author

*E-mail: okarlstr@abo.fi.

ACKNOWLEDGMENTS

This research was funded by Tekes within the ERANET/Bioenergy project: Science Tools for Fuel Characterization for Clean and Efficient Biomass Combustion (SciToBiCom), Nordic Graduate School of Biofuel Science and Technology-2, and by Chemcom, which is a mainly Tekes funded project co-ordinated by the Process Chemistry Centre (PCC) at Åbo Akademi University in Turku, Finland. PCC is a Centre of Excellence appointed by the Academy of Finland. Other Chemcom partners are Andritz Oy, Foster Wheeler Energia Oy, International Paper Inc., Metso Power Oy, Oy Metsä-Botnia Ab, Clyde Bergemann GmbH, and UPM-Kymmene

Oyj. The authors extend thanks to the International Flame Research Foundation (IFRF) Members' Research Program, which made the IFRF Solid Fuel Database available for this study.

REFERENCES

- (1) Williams, A.; Pourkashanian, M.; Jones, J. M. *Prog. Energy Combust. Sci.* **2001**, *27*, 587–610.
- (2) Smith, I. W. *19th Symp. (Int.) Combust.* **1982**, 1045–1065.
- (3) Petersen, E. E. *AIChE J.* **1957**, *3*, 443–449.
- (4) Bhatia, S. K.; Perlmutter, D. D. *AIChE J.* **1980**, *26*, 379–386.
- (5) Feng, B.; Bhatia, S. K. *Carbon* **2003**, *41*, 507–523.
- (6) Mitchell, R. E.; Ma, L.; Kim, B. *Combust. Flame* **2007**, *151*, 426–436.
- (7) Phillips, R.; Vastola, F. J.; Walker, P. L. Jr. *Carbon* **1969**, *7*, 479–485.
- (8) Walker, P. L. Jr.; Taylor, R. L.; Ranish, J. M. *Carbon* **1991**, *29*, 411–421.
- (9) Hurt, R. H.; Haynes, B. S. *Proc. Combust. Inst.* **2005**, *30*, 2161–2168.
- (10) Murphy, J. J.; Shaddix, C. R. *Combust. Flame* **2006**, *144*, 710–729.
- (11) Hurt, R.; Sun, J.-K.; Lunden, M. *Combust. Flame* **1998**, *113*, 181–197.
- (12) Ballester, J.; Jiménez, S. *Combust. Flame* **2005**, *142*, 210–222.
- (13) Williams, A.; Backreedy, R.; Habib, R.; Jones, J. M.; Pourkashanian, M. *Fuel* **2002**, *81*, 605–618.
- (14) Baum, M. M.; Street, P. J. *Combust. Sci. Technol.* **1971**, *3*, 231–243.
- (15) Hurt, R. H.; Calo, J. M. *Combust. Flame* **2001**, *125*, 1138–1149.
- (16) Fennel, P. S.; Dennis, J. S.; Hayhurst, A. N. *Proc. Combust. Inst.* **2009**, *32*, 2051–2058.
- (17) Haykırı-Açma, H.; Ersoy-Meriçboyum, A.; Küçükbayrak, S. *Energy Convers. Manage.* **2001**, *42*, 11–20.
- (18) Hargrave, G.; Pourkashanian, M.; Williams, A. *21st Symp. (Int.) Combust.* **1986**, 221–230.

- (19) Levenspiel, O. *The Chemical Reactor Omnibook*; Oregon State University Bookstores: Corvallis, OR, 1996.
- (20) Field, M. A. *Combust. Flame* **1970**, *14*, 237–248.
- (21) Hurt, R. H.; Mitchell, R. E. *24th Symp. (Int.) Combust.* **1992**, 1243–1250.
- (22) Smith, I. W. *Fuel* **1978**, *57*, 409–414.
- (23) Smooth, L. D.; Smith, P. J. *Coal Combustion and Gasification*; Plenum Press: New York, 1985; p 85.
- (24) Smith, I. W. *Combust. Flame* **1971**, *17*, 421–428.
- (25) Karlström, O.; Brink, A.; Hupa, M.; Tognotti, L. *Combust. Flame* **2011**, *158*, 2056–2063.
- (26) Charpenay, S.; Serio, M. A.; Salomon, P. R. *24th Symp. (Int.) Combust.* **1992**, 1189–1197.
- (27) Fu, W. B.; Chang, B. L.; Zheng, S. M. *Combust. Flame* **1997**, *109*, 587–598.
- (28) Zolin, A.; Jensen, A. D.; Jensen, P. A.; Dam-Johansen, K. *Fuel* **2002**, *81*, 1065–1075.
- (29) Essenhigh, R. H. Fundamentals of coal combustion. In *Chemistry of Coal Utilization*; Elliott, M. A., Ed.; John Wiley & Sons: New York, 1981; Ch. 19.
- (30) Hercog, J.; Tognotti, L. *Realization of IFRF Solid Fuel Database*, IFRF Doc No. E36/y/02; International Flame Research Foundation: Tuscany, Italy, 2008.
- (31) Kalinchak, V. V.; Dubinkii, A. V. *J. Eng. Phys. Thermophys.* **1995**, *4*, 470–475.
- (32) Tognotti, L.; Longwell, J. P.; Sarofim, A. F. *Twenty-third Symp. (Int.) Combust.* **1990**, 1207–1213.
- (33) Essenhigh, R. H. *Sixteenth Symp. (Int.) Combust.* **1976**, 353–374.
- (34) Haas, J.; Weber, R. J. *Energy Inst.* **2010**, *83*, 225–234.
- (35) Brix, J.; Jensen, P. A.; Jensen, A. D. *Fuel* **2011**, *90*, 2224–2239.